UNIVERSIDADE DE SÃO PAULO

PUBLICAÇÕES

SINGLE GRADED-RESPONSE NEURON MODEL WITH RECURRENT EXCITATION: DISTRIBUTED DELAY

K. Pakdaman[1], C.P. Malta[2], C. Grotta-Ragazzo[3] , and J.-F. Vibert[1]

[1]B3E, INSERM U 444, ISARS
Falcuté de Médecine Saint-Antoine
27, rue Chaligny, 75571 Paris Cedex 12, FRANCE

[2]Instituto de Física, Universidade de São Paulo

[3]Instituto de Matemática e Estatística
Universidade de São Paulo
CP 66281, 05389-970, São Paulo, BRASIL

Determination of the Electric Field Gradient Tensor by 2D NQR

Hernán Cervantes R.*, Said R. Rabbani

Instituto de Física, Universidade de São Paulo, Caixa Postal 66318,
CEP 05389-970 São Paulo, SP, Brazil.

Christovam Mendonça

Departamento de Física, Universidade Federal de São Carlos, CEP 13565-905 São Carlos, SP, Brazil.
(November 13, 1996)

For a full specification of the Electric Field Gradient (EFG) tensor five independent parameters are necessary: the asymmetry parameter (η), the largest component of the EFG (eq), and three angles which determine the orientation of the EFG principal axis in respect to the crystallographic frame. eq and η can be determined independently by pure Nuclear Quadrupole Resonance (NQR) (only for nuclear spin $I > 3/2$). However, to determine the orientational angles one needs to use other methods such as X-Ray Crystallography, Nuclear Magnetic Resonance (NMR), NQR with external field, EPR, Mössbauer spectroscopy or Perturbed Angular Correlations (PAC). In this letter we propose a new 2D NQR method which permits the full determination of the EFG tensor in a monocrystalline sample. It also can be used to determine the preferential orientation of small monocrystals in a polycrystalline sample. The best angular precision of the method is $\pm 2.5°$

PACS number: 76.60.Gv

The two dimensional spectroscopy is a relatively new technique which was introduced by Jeener [1,2]. This technique explores the possibility of manipulating the spin Hamiltonian in such a way that it has different forms during the period of evolution, t_1, and the data acquisition time, t_2, Fig. 1. Therefore, the Free Induction Decay (FID) $S(t_1, t_2)$, depends on two variables t_1 and t_2. There are several procedures by which the two dimensional spectra can be obtained from $S(t_1, t_2)$ [2-4]. While the two dimensional NMR spectroscopy is widely used in a variety of applications, the 2D NQR spectroscopy is relativity new and only recently started to have some applications such as spatially resolved NQR spectra (NQR imaging) [4-11], nutation NQR spectroscopy [3,12,13] and 2D exchange NQR spectroscopy [14,15].

In this Letter, we show the possibility of using a two dimensional NQR method to determine the EFG tensor in a crystallographic frame in a very straightforward way. Up to now this determination has been performed by using a variety of techniques which either are very expensive or otherwise very tedious [16,17,20,18,19].

If a crystal orientation in a rf coil is such that the coil axis make an azimuthal angle ϕ and polar angle θ with respect to the EFG coordinate, the induced signal in the coil, due to one nuclei ($I = 3/2$) a time t' after a pulse of duration t_w, can be written as [21] :

$$G(t', t_w, \theta, \phi) \sim R(\theta, \phi) \sin \left\{ \frac{\omega_1 t_w}{2\sqrt{3}a} R(\theta, \phi) \right\} \sin \omega_0 t' \tag{0.1}$$

where
$a = \sqrt{1 + \eta/3}$,
$R(\theta, \phi) = \sqrt{4\eta^2 \cos^2 \theta [9 + \eta^2 + 6\eta \cos(2\phi)] \sin^2 \theta}$,
$\omega_1 = \gamma H$ is the Larmor frequency, and
ω_0 is the quadrupole resonance frequency.
For $\eta = 0$, equation (0.1) can be written as

$$G(t', t_w, \theta) \sim \sin \theta \sin(\omega_N t_w \sin \theta) \sin \omega_0 t' \tag{0.2}$$

where $\omega_N = \frac{\omega_1}{2\sqrt{3}}$ is called the nutation frequency.

For a system of randomly oriented spins the total signal induced in the probe coil is proportional to the integral of the equation (0.2) over the unitary sphere. However, for a monocrystalline sample where the orientation of the EFG principal axis has a narrow distribution, $n(\theta)$, around θ, the rf coil polar angle in EFG coordinate, the signal in the probe coil should be written as

$$G(t', t_w) \sim Q(t') \sin \omega_0 t' \int_0^\pi n(\theta) \sin^2 \theta \sin(\omega_N t_w \sin \theta) d\theta$$

where $Q(t')$ is related to the system relaxation.

By Fourier transformation of $G(t', t_w)$ with respect to t' we obtain

$$G(\omega', t_w) \sim \Im[Q](\omega') \int_0^\pi n(\theta) \sin^2 \theta \sin(\omega_N t_w \sin \theta) d\theta.$$

One can obtain an expression for the pseudo-FID (pFID) by fixing the value of ω'

$$S(t_w) = G(\omega' = const, t_w) \sim$$

$$\sim \int_0^\pi n(\theta) \sin^2 \theta \sin(\omega_N t_w \sin \theta) d\theta \tag{0.3}$$

The distribution $n(\theta)$ can be obtained from the expression of pFID by the Maximum Entropy Method (MEM)

[22]. In this case, the signal induced in the probe coil is written as

$$S_p = \sum_{j=1}^{M} n_j D_{p,j} + \omega_p, \quad 1 \leq p \leq N$$

where

$D_{p,j}$ are the transference matrix coefficient,

$$D_{p,j} = \sin^2 \theta_j \sin(\omega_N t_p \sin \theta_j),$$

$\{n_j = n(\theta_j)\}_{1 \leq j \leq M}$ is the true distribution, and

ω_p, which represent the noise, is a Gaussian process with zero mean and standard deviation σ_p.

The signal, estimated by a given set $\{X_j\}_{1 \leq j \leq M}$ of positive numbers, satisfying the condition $\sum_{j=1}^{M} X_j = 1$, can be written in the following way:

$$\widetilde{S}_p = \sum_{j=1}^{M} X_j D_{p,j}, \quad p = 1, 2, .., N \qquad (0.4)$$

Using MEM, it is possible to choose a set of positive numbers, $\{X_j\}$, so that the estimated signal (0.4) reproduce the experimental data, S_p.

The best set is the one that minimizes the *entropy* function

$$H = -\sum_{j=1}^{M} X_j \ln X_j \qquad (0.5)$$

subject to the constraint of the compatibility with the experimental data, i.e.,

$$\chi^2 = \sum_{p=1}^{N} \frac{(S_p - \widetilde{S}_p)^2}{\sigma^2} \leq N \qquad (0.6)$$

and

$$\sum_{j=1}^{M} X_j = 1 \qquad (0.7)$$

Numerical simulations has been made to test the method. The pseudo-FID was obtained by numerical integration of the equation (0.3) assuming a Gaussian distribution for $n(\theta)$, plus 10% of Gaussian noise.

Result of the deconvolution is shown in Fig. 2(a), the full line represents the assumed distribution and the dots line represents the calculated distribution using the MEM. The corresponding pFIDs are shown in Fig. 2(b). Both distributions are normalized with the criterium (0.7). The error bars represent the standard deviation of the noise, $\sigma = 0.1$. The numerical values are pointed out in Table I.

In Fig. 3(a) we present the result for another case, where the true distribution $n(\theta)$ is now taken as the sum of two Gaussians (solid line). The result of the deconvolution is represented by the dots line. Fig. 3(b) shows the

corresponding pFIDs. The distribution satisfies equation (0.7) and the error bars are the noise standard deviation. The numerical values are shown in Table II.

Other simulations were performed for $n(\theta) = const$ and $n(\theta) = const$ plus Gaussian distribution, in both cases we were able to extract the assumed distribution using our method.

The method was used to determine the direction of V_{zz} in Sodium Chlorate sample $(NaClO_3)$. $NaClO_3$ has a cubic structure with one molecule of $NaClO_3$ per cell, and belongs to the symmetry group T^4 with V_{zz} oriented along the principal diagonal of the cube [23].

The monocrystalline samples were obtained by slow evaporation of the saturated solution of highly pure $NaClO_3$ in bidestilated water.

The geometric form of the monocrystal was used for the orientation of the sample in the coil. In the first experiment the coil axis lies in the direction [001] and in the second experiment it lies in the direction [111]. In the first case the four diagonals make an angle of $0,9553$ *radian* (54°44'8,2") with the coil axis. In the second case the coil makes an angle of $1,2309$ *radian* (70°31'43,61") with three diagonals and 0 *radian* with the other.

The experimental data were obtain using a computer-controlled pulse NQR spectrometer as described previously in detail [24]. The NQR spectra were obtained for a series of different pulse duration through FFT of Free Induced Decay (FID) following each pulse. In order to improve the signal to noise ratio, for each pulse duration, 32 FID's were averaged out to produce the final FID. Finally, the NQR line amplitude for different pulses were plotted versus duration of each pulse. This graph represents our experimental pFID. The pulse duration varied from $2\mu s$ to $100\mu s$ with an increment of $2\mu s$. The only unknown parameter, the nutation frequency ω_N, was obtained by fitting a pFID of a polycrystalline sample to the equation (0.3) with $n(\theta) = const$.

Fig. 4(a) shows the distribution obtained by deconvolution of the experimental pFID using MEM in the first experiment and the Fig. 4(b) shows the experimental pFID, in full line, and estimated pFID, in dots line. The error bars are the estimated experimental error. The expected and calculated numerical values are presented in Table III.

The result of the second experiment are shown in Figs. 5(a) and 5(b). The numerical values are represented in Table IV.

In conclusion, the method we have presented makes possible the determination of the EFG tensor in crystalline frame for monocrystalline samples using pure NQR nutation spectroscopy in a new fashion.

2

* To whom the correspondence should addressed. Electronic address : hernan@fge.if.usp.br

[1] Jeener, Lectures, Ampère International Summer School, Basko Potze, Yugoslavia (1971) unpublished.

[2] Ernest et al., in *Principles of NMR in One and Two Dimensions*, (Clarendon Press, Oxford, 1991) p. 283.

[3] G. Harbinson, A. Slokenberg, and T. Barbara, J. Chem. Phys. **90**, 5292 (1989).

[4] H. Robert, A. Minuzzi, and J. Pusiol, J. Magn. Reson. A **118**, 189 (1996).

[5] S. Matsui, K. Kose, and T. Inouye, J. Magn. Reson. **88**, 186 (1990).

[6] K. Ermolaev et al., Appl. Magn. Reson. **2**, 683 (1991).

[7] R. Kimmich et al., Z. Naturforsch. **47a**, 361 (1992).

[8] P. Nickel et al., Chem. Phys. Lett. **183**, 183 (1991).

[9] R. Kimmich, E. Rommel, and P. Nickel, Magn. Reson. Imaging **10**, 733 (1992).

[10] P. Nickel et al., J. Magn. Reson. A **111**, 191 (1994).

[11] E. Rommel et al., J. Magn. Reson. **91**, 630 (1991).

[12] H. Robert et al., Z. Naturforsch. **49a**, 35 (1994).

[13] J. Dolinšek et al., J. Magn. Reson. A **114**, 147 (1995).

[14] E. Rommel et al., Z. Naturforsch. **47a**, 382 (1992).

[15] P. Nickel, and R. Kimmich, J. Mol. Structure **345**, 253 (1995).

[16] A. Ayala, R. Alonso, and A. López-García, Phys. Rev. B **50**, 3547 (1994).

[17] U. Gonser, in *Proceedings of the School an Applications of Nuclear Gamma Resonance Spectroscopy (Mössbauer Spectroscopy), Trieste, 1986*, edited by N. Eissa, and G. Denaro, (Word Scientific) p. 1.

[18] A. Abragam, in *The Principles of Nuclear Magnetism*, edited by (Oxford University Press , 1994) , p. 236.

[19] W. Witthuhn, and W. Engel, in *Hyperfine Interactions of Radioactive Nuclei*, edited by J. Christiansen (Springer-Verlag, 1983) p. 205.

[20] A. Brown, and M. Spackman, Mol. Phys. **83**, 551 (1994).

[21] J. Pratt, Molecular Phys. **34**, 539, 1977.

[22] E. Jaynes, Physics Rev. **106**, 620, 1957.

[23] H. Zeldes, and R. Livingston, J. Chem. Phys. **26**; 1102, 1957.

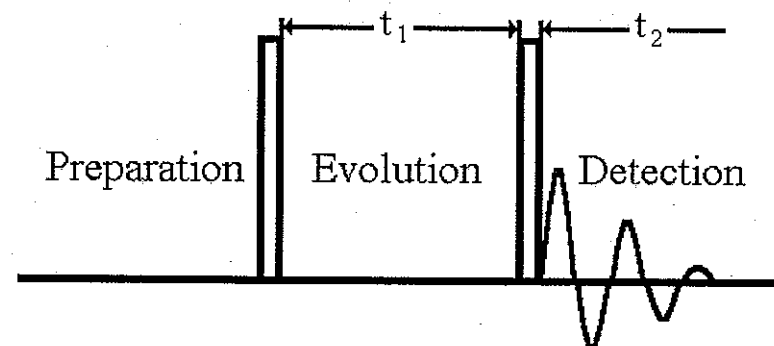[24] S. Rabbani et al., Phys. Rev. B **51**, 8848 (1995).
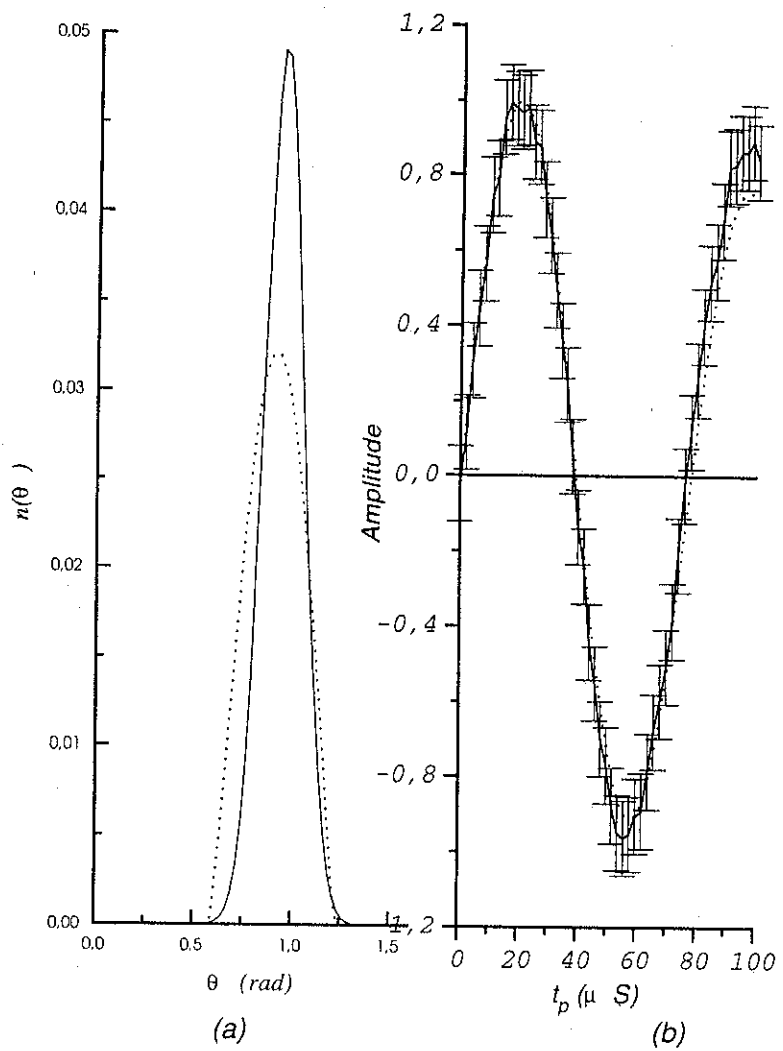
FIG. 1. Basic scheme for 2D time-domain spectroscopy.

FIG. 2. FIRST SIMULATION. (a) EFG principal axes distribution used (solid line) and deconvoluted by MEM (dots line) ᵗith one peak. (b) pFID simulated plus noise of $\sigma = 0,1$ (solid) line, and estimated one (dots line).
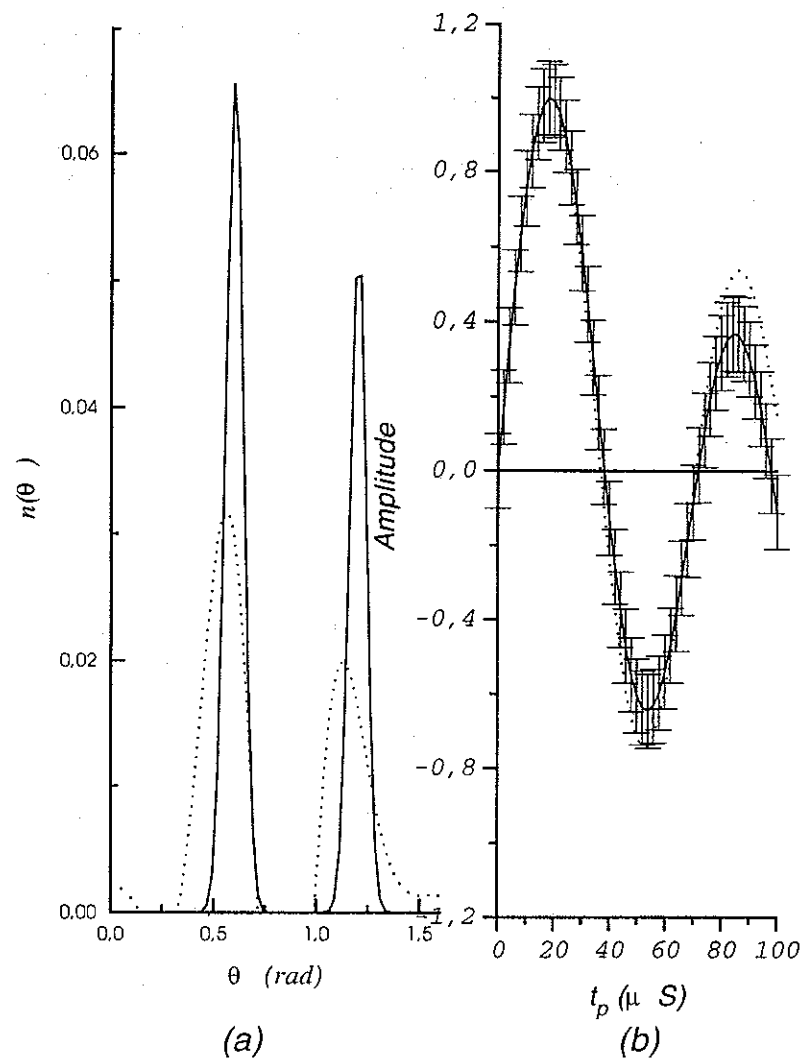

FIG. 3. SECOND SIMULATION. (a) Used to simulate the pFID (solid line), and deconvoluted distribution obtaineɪ MEM (dots line). (b) Simulated pFID (solid line) and the error bars with $\sigma = 0,1$ (solid line) and estimated pFID (dots ɪ
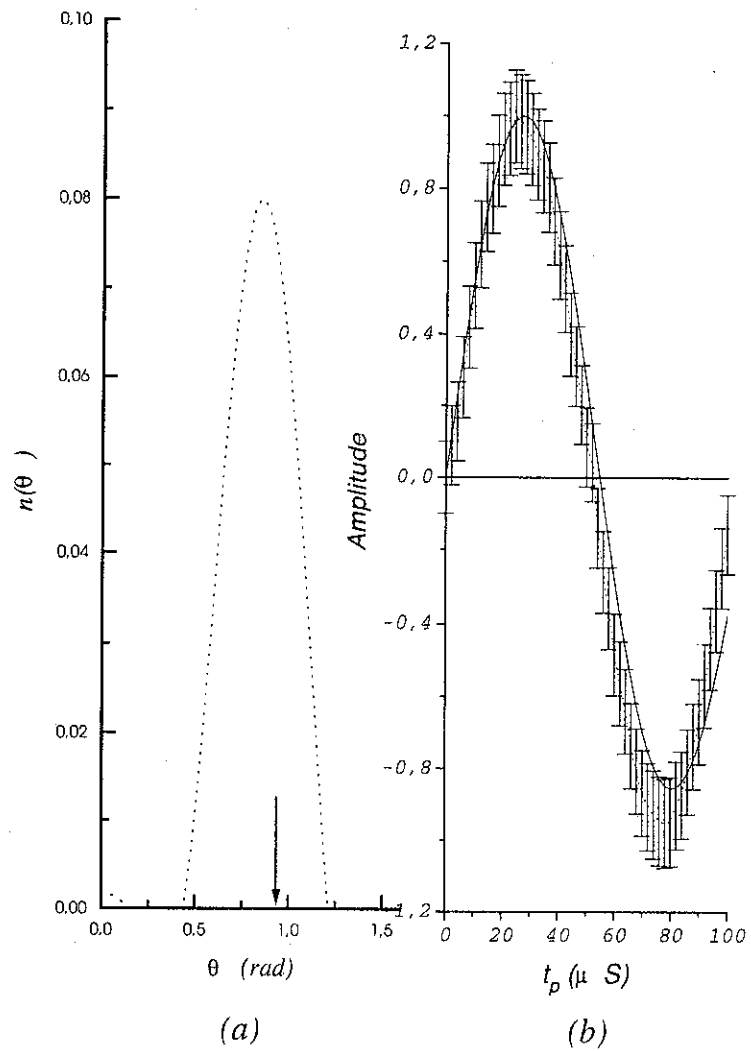
FIG. 4. FIRST EXPERIMENT. Coil axis in the direction [001]. (a) Distribution deconvoluted by MEM (dots line). The arrow represents the expected direction of V_{zz}. (b) Both pFID, experimental and experimental error, (solid line) and the estimated pFID (dots line). The error bars are the estimated experimental error.
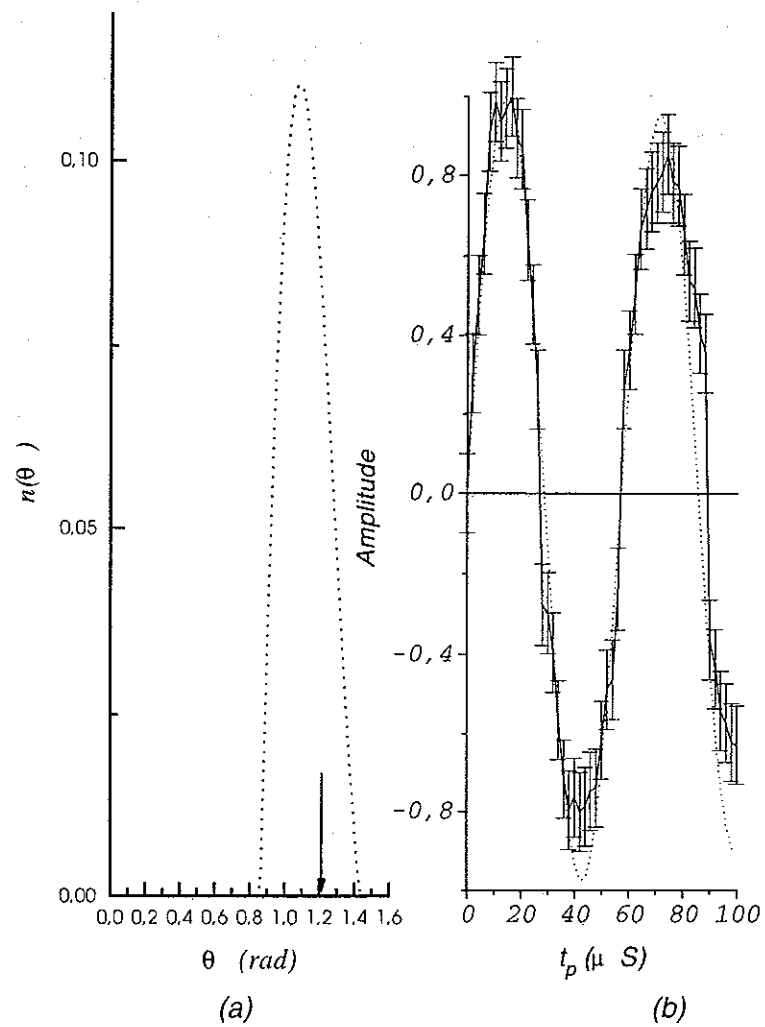

FIG. 5. SECOND EXPERIMENT. Coil axis in the direction [111]. (a) Distribution deconvoluted by MEM. The ; represents the expected direction of V_{zz}. (b) Experimental pFID and experimental error (solid line), and estimated pFID line). The error bars represent the estimated experimental error.

TABLE I. FIRST SIMULATION. Numerical values used for simulation and the ones obtained by MEM.

	Center	Half width
Used in the simulation	0,95	0,2
Estimated by MEM	0,91476	0,30193
Relative error	0,037	0,51

TABLE II. SECOND SIMULATION. Numerical values used to simulate the pFID and the ones obtained using MEM.

	Center	Half width	peak ratio
Used	.		1:0,75
Peak 1	0,60	0,085	
Peak 2	1,20	0,080	
Estimated by MEM			1:0,67
Peak 1	0,55004	0,17536	
Peak 2	1,2533	0,19133	
Relative Error			0,11
Peak 1	0,083	1,06	
Peak 2	0,039	1,39	

TABLE III. FIRST EXPERIMENT. Numerical values expected and the ones obtained by MEM.

	Center	Half width
Expected	0,95532	-
Estimated by MEM	0,97606	0,12796
Relative Error	0,022	-

TABLE IV. SECOND EXPERIMENT. Numerical values expected and the ones obtained by MEM.

	Center	Half width
Expected	1,2309	-
Estimated by MEM	1,1022	0,26824
Relative Error	0,1046	-